Hydrogen Bond Dynamics at the Water/Hydrocarbon Interface†

Janamejaya Chowdhary* and Branka M. Ladanyi*

Department of Chemistry, Colorado State University, Fort Collins, Colorado 80523-1872

Received: July 11, 2008; Revised Manuscript Received: September 12, 2008

The dynamics of hydrogen bond formation and breakage for water in the vicinity of water/hydrocarbon liquid interfaces is studied using molecular dynamics simulations. Several liquid alkanes are considered as the hydrocarbon phase in order to determine the effects of their chain length and extent of branching on the properties of the adjacent water phase. In addition to defining the interface location in terms of the laboratory-frame density profiles, the effects of interfacial fluctuations are considered by locating the interface in terms of the proximity of the molecules of the other phase. We find that the hydrogen bond dynamics of interfacial water is weakly influenced by the identity of the hydrocarbon phase and by capillary waves. In addition to calculating hydrogen bond time correlations, we examine how the hydrogen bond dynamics depend on local coordination and determine the extent of cooperativity in the population relaxation of the hydrogen bonds that a given molecule participates in. The contributions of translational diffusion and reorientation of molecular O−H bonds to the mechanism of hydrogen bond breakage and reformation are investigated. In previous work, we have shown that rotation of the principal axes of water is anisotropic at the interface and depends on the initial orientation of the molecule relative to the interface. Here, we extend this analysis to the reorientation of the O−H vector and to hydrogen bond time correlation. We find that hydrogen bond dynamics are also sensitive to the initial orientation of the molecules participating in the hydrogen bond.

I. Introduction

The unique properties of water are a consequence of its hydrogen bonded network. Dynamics are governed by the elementary process of hydrogen bond formation and breakage, and this has been extensively studied via computer simulations[1−7] and experiments such as 2-D infrared spectroscopy.[8,9] The physical picture that emerges from various studies of water under ambient conditions is that of diffusion of a molecule into the first coordination shell of a central water molecule and the formation of a five coordinated short-time intermediate state. The intermediate state is associated with the transfer of one O···H bond from the old hydrogen bond acceptor to the new molecule, and transfer of the hydrogen bond involves an angular jump for the O−H covalent bond and a slow network rearrangement.[9,10] The overall process is cooperative, and dynamics of hydrogen bonds within the network are correlated.[6,11]

While most studies have focused on bulk water, the presence of an interface disrupts the structure and dynamics of the hydrogen bonded network. For aqueous interfaces, the average number of hydrogen bonds made by a water molecule with other water molecules decreases from ∼3.5 in the bulk to ∼2.0 at the interface, although hydrogen bonding is more efficient in maximizing the number of hydrogen bonds with the available neighbors.[12−14] Associated with this change in the nature of hydrogen bonding at the interface, hydrogen bond dynamics are faster than in the bulk at the air/water interface[15] but slower than in the bulk at the interface of water with metals,[16] organic liquids,[12] surfactant monolayers,[17] and carbon nanotubes.[18]

In recent work, we have examined the structure[13] and single molecule relaxation[19] at water/hydrocarbon interfaces in order to identify the effect of hydrocarbon branching and surface fluctuations on interfacial properties. For water, single molecule dynamics revealed weak dependence on hydrocarbon branching. Furthermore, the dynamics were more anisotropic than bulk liquid and orientational relaxation was found to depend on the initial orientation of the molecules at the interface for both liquids. Our objective here is to understand how a more collective dynamical property, hydrogen bond population relaxation, is affected by hydrocarbon branching, surface fluctuations, and initial orientation of the interfacial water molecules. Section II contains a brief description of the simulation methods and system setup. In section III, we present our results on different ways of quantifying hydrogen bond dynamics and the observed variation between bulk and interfacial regions of our system. Finally, in section IV, we present a summary of our results.

II. Simulation Method, Interaction Model, and Hydrogen Bond Definition

The simulation methodology is summarized here and presented in detail elsewhere.[13] Molecular dynamics (MD) simulations are performed at 298 K and 1 atm for interfacial systems formed by SPC/E water[20] with the five hydrocarbons: *n*-pentane (P), 2-methyl pentane (2MP), 2,2,4-trimethyl pentane (TMP), 2-methyl heptane (2MH), and *n*-octane (O). The united atom OPLS force field[21] was used to model the hydrocarbon. The number of water molecules was kept fixed at 586, and the number of hydrocarbons was selected to be 182, 158, 128, 128, and 128 for P, 2MP, TMP, 2MH, and O, respectively. This system was configured so as to have the water phase in the middle with the hydrocarbon molecules on either side. The two interfaces formed are in the (x, y) plane so that density variation is along the z-axis. A time step of 2 fs was used to integrate the equations of motion, and configurations are saved every 10 time steps corresponding to an interval of 20 fs.

† Part of the special section "Aqueous Solutions and Their Interfaces".

* Author to whom correspondence should be sent. E-mail: janamejaya.chowdhary@gmail.com and Branka.Ladanyi@colostate.edu.

10.1021/jp8061509 CCC: $40.75
Published on Web 11/20/2008

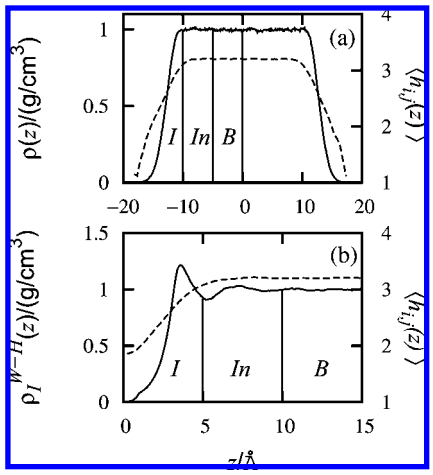

Figure 1. Density profile (solid line) and hydrogen bond profile (dashed line) for the water phase in the water/TMP system (a) laboratory frame and (b) intrinsic frame. The partitions of the aqueous phase in each frame are labeled *I*, *In*, and *B* for interfacial, intermediate, and bulk.

The laboratory-frame density profile for water is calculated on the basis of the position of the oxygen atom for each water molecule and presented in Figure 1a. The presence of capillary waves at the interface broadens any intrinsic structure and leads to the laboratory-frame density profile. In order to minimize the effect of capillary waves, we study aqueous structure with respect to the reference surface defined by the outermost hydrocarbon sites, i.e., the intrinsic frame. On the basis of a procedure described elsewhere,[13] the set of hydrocarbon sites at the interface is identified. Then, for the set of hydrocarbon surface sites $\{\xi(\mathbf{R})\}$ at a mean height of z_0, each surface site is projected onto the (x, y) plane and a Voronoi tesselation of the (x, y) plane is performed. Every oxygen atom is then projected onto the (x, y) plane and assigned to the hydrocarbon site that occupies the Voronoi polygon the oxygen atom projects into. The difference in heights of the hydrocarbon surface site and the oxygen atom then is an approximation to the distance of the oxygen atom from the reference surface in the intrinsic frame. The intrinsic density profile so constructed with respect to the hydrocarbon surface[13] is presented in Figure 1b.

In order to distinguish between the interfacial and bulk water phases, we partition the aqueous phase in the laboratory frame into six regions of 5 Å width. Molecules in the two regions -15 Å $< z < -10$ Å and 10 Å $< z <$ 15 Å were identified as interfacial water ($k = 1$), those in the regions -5 Å $< z < 0$ Å and 0 Å $< z <$ 5 Å were identified as bulk water ($k = 3$), and the remaining molecules were categorized as intermediate ($k = 2$), where the value of k indicates the type of water molecule. Just as for the laboratory frame, the water layer was partitioned into three regions with 5 Å width in the intrinsic frame. Molecules in the region 0 Å$< z <$ 5 Å, 5 Å $< z <$ 10 Å, and 10 Å $< z <$ 15 Å are categorized as interfacial ($k = 1$), intermediate ($k = 2$), and bulk ($k = 3$). With this classification of water molecules into interfacial, intermediate, and bulk, we present our analysis of hydrogen bond dynamics in the following sections.

To characterize the hydrogen bond network, a pair of water molecules is considered to be hydrogen bonded if the O−O distance is smaller than 3.5 Å and the O−O−H angle is smaller than $\pi/6$.[4] The hydrogen bonded state of an instantaneous configuration is characterized by the variable $h_{i,j}(t)$ which takes a value of 1 or 0 at time t depending on whether the molecules i and j are hydrogen bonded or not. In order to correct for the finite size of the system, we calculate the average number of hydrogen bonds per molecule in a given region as

$$\tilde{h}_k = \langle \sum_{(i\neq j)\in k} h_{i,j}/N_k^2 \rangle \tag{1}$$

where N_k is the number of molecules in region k and $\langle ... \rangle$ indicates an ensemble average.

A key structural characteristic of the hydrogen bonded network is the average number of hydrogen bonds per molecule, $\langle h_{i,j} \rangle$. For all interfacial systems, we find the average number of hydrogen bonds in the bulk phase is ∼3.2 which is slightly lower than the usual estimate of 3.4 for SPC/E water. In a previous calculation,[13] due to an error in hydrogen bond identification, we found about 3.8 hydrogen bonds per molecule and this has been corrected here. A decrease from 3.2 occurs primarily in the interfacial region, as revealed by the hydrogen bond profile in the laboratory and intrinsic frames in Figure 1. A key difference in the laboratory and intrinsic hydrogen bond profiles is that the number of hydrogen bonds formed by water molecules farthest from the bulk phase is 1.1 in the laboratory frame and 1.9 in the intrinsic frame. This difference can be rationalized in terms of the broadening of the intrinsic profile due to capillary waves.

While not presented here, the efficiency of hydrogen bonding, as characterized by the percentage of available neighboring molecules that are involved in hydrogen bonding, improves at the interface.[13] This tendency to form a more efficiently hydrogen bonded network at the interface is accompanied by slower single molecule relaxation at the interface, thereby connecting local structure to dynamics.[19]

III. Hydrogen Bond Dynamics

A. Hydrogen Bond Time Correlation Function. On the basis of the criterea for hydrogen bonding defined in section II, all hydrogen bonded pairs of water molecules are identified for each configuration. The finite-size correction for each region of the aqueous phase is calculated using eq 1, and hydrogen bond dynamics can be studied in terms of the variable $h_{i,j}(t) - \tilde{h}_k$. We calculate the following time correlation function (TCF)[3,4]

$$H_k(t) = \frac{\langle [h_{i,j}(t) - \tilde{h}_k][h_{i,j}(0) - \tilde{h}_k] \rangle}{\langle [h_{i,j}(0) - \tilde{h}_k]^2 \rangle} \tag{2}$$

which corresponds to the probability that a pair of molecules hydrogen bonded at time $t = 0$ remain hydrogen bonded at time t irrespective of hydrogen bond breakage prior to time t. The correlation function was calculated for all water/hydrocarbon systems and different regions of the aqueous phase.

We present our results for $H_k(t)$, in the laboratory frame, in Figure 2a for interfacial, intermediate, and bulk water phase regions of the water/TMP system. The correlation functions for the bulk and the intermediate water regions are almost identical. Interfacial water exhibits slower relaxation, indicating slower hydrogen bond dynamics at the interface. While not shown, the same trend is observed for all water/hydrocarbon systems.

The time dependence of the correlation function is best fit to the stretched exponential

$$H_k(t) = a_r \exp[-(t/\tau_r)^{\gamma_r}] \tag{3}$$

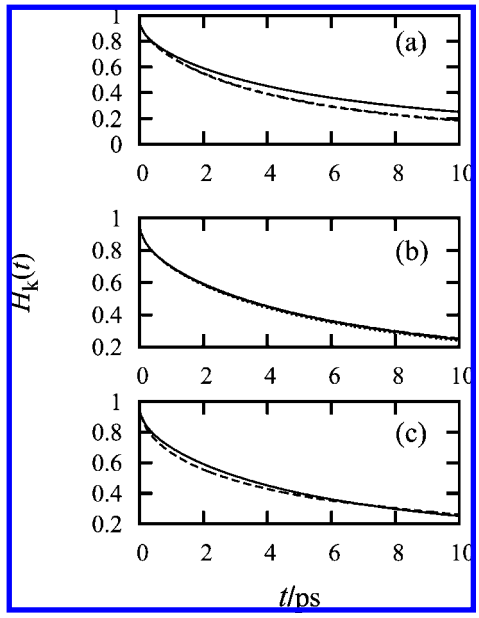

Figure 2. Hydrogen bond time correlation function, $H_k(t)$, for (a) interfacial (solid), intermediate (large dashes), and bulk water (small dashes) for the water/TMP system in the laboratory frame, (b) interfacial water for all five interfacial systems—P (solid), 2MP (large dashes), TMP (small dashes), 2MH (dashed dot), and O (dotted line)—in the laboratory frame, and (c) interfacial water for the water/TMP interface in the laboratory (solid) and intrinsic (large dashes) frames.

TABLE 1: Parameters for the Fit of the Laboratory-Frame Hydrogen Bond Time Correlation, $H_k(t)$, to eq 3 Where τ_r Has Units of Picoseconds

	bulk		intermediate		interfacial	
hydrocarbon	τ_r	γ_r	τ_r	γ_r	τ_r	γ_r
P	4.65	0.68	4.68	0.69	6.03	0.64
2MP	4.68	0.68	4.71	0.67	6.23	0.64
TMP	4.78	0.68	4.68	0.68	6.32	0.64
2MH	4.82	0.67	4.79	0.67	6.35	0.65
O	4.94	0.68	4.86	0.67	6.35	0.64

and the parameters are presented for all water/hydrocarbon systems in Table 1. For the bulk phase, the relaxation time τ_r is of the order of ~4.8 ps for all interfacial systems and is larger than the value of 4.2 ps reported for SPC/E water by Xu et al.[22] (they define $H_k(\tau_r) = 1/e$) but slightly smaller than the value of ~5 ps reported by Starr et al.[7] for the same water model. The exponent γ_r has a constant value of 0.68 for all systems and is comparable to the value of 0.66 obtained by Starr et al.[7] Hydrogen bond dynamics in the bulk phase is independent of the hydrocarbon phase, as expected.

Corresponding to the overlapping TCFs for the bulk and intermediate water regions in Figure 2a, the relaxation time τ_r and exponent γ_r for these two regions are also similar. The largest change in fit parameters occurs at the interface where τ_r increases by ~1.5 ps with respect to bulk water. Since hydrogen bond dynamics is related to translational and rotational motion which are slower at the interface, we should expect τ_r to increase at the interface.[19] The change in γ_r from 0.68 to 0.64 is indicative of a slightly broader distribution of time scales associated with hydrogen bond dynamics at the interface with respect to bulk.

Turning to the dependence of hydrogen bond dynamics at the interface on the hydrocarbon phase, the time evolution of $H_k(t)$ for interfacial water in the laboratory frame is presented in Figure 2b for all systems. The corresponding relaxation times for the five interfacial systems are presented in Table 1 and show larger variation in τ_r than in the bulk-like region. In the interfacial region, the decay of $H_k(t)$ slows down on going from P to 2MP to TMP with τ_r increasing from 6.03 to 6.32 ps, indicating slightly faster dynamics near smaller hydrocarbon molecules. For TMP, 2MH, and O (same mass, different extent of branching), the relaxation times show a slight increase with chain length. These observations indicate a weak dependence of interfacial hydrogen bond dynamics on the hydrocarbon phase. Since we did not find a significant effect of hydrocarbon branching on water structure and single molecule dynamics,[19] this observation is not surprising.

At the liquid/liquid interface, the capillary waves[23,24] broaden the two liquid surfaces forming the interface, thereby leading to an additional contribution to dynamics. The effect of capillary waves can be minimized by applying a weak external field[12] or by studying properties of the liquid as a function of distance from the surface of the other liquid forming the interface, i.e., the intrinsic property. We have studied interfacial structure and single molecule dynamics in the intrinsic frame before,[19] and here, we calculate $H_k(t)$ for molecules within 5 Å from the hydrocarbon surface at the interface. The correlation function for interfacial water is presented for the water/TMP system in Figure 2c along with the laboratory-frame data. The decay of $H_k(t)$ is slightly faster in the intrinsic frame than in the laboratory frame. Fitting to eq 3 gives a relaxation time of 5.63 ps in the intrinsic frame which is smaller than the value of 6.32 in the laboratory frame and suggests weak sensitivity of hydrogen bond dynamics to capillary wave fluctuations at the interface.

B. Cooperativity and Dependence on Local Environment. A key feature of the hydrogen bond TCFs presented in the previous section is their nonexponential character. If the relaxation of a hydrogen bond made by a given molecule were independent of the other hydrogen bonds made by the same molecule and other processes occurring on the same time scale, first order kinetics would be expected and the long-time behavior of the TCF would be exponential.[2−4] We do not observe exponential decay of $H_k(t)$ and proceed now to identify the molecular mechanisms that contribute to this behavior. One possible origin for the observed nonexponential decay of $H_k(t)$ could be the cooperativity of hydrogen bond relaxation.

We study the extent of cooperativity in hydrogen bond dynamics by calculating the following family of correlation functions

$$Q_k^n(t) = \langle \prod_{x=1}^{n} [h_{i,x}(t) - \tilde{h}_k][h_{i,x}(0) - \tilde{h}_k] \rangle \qquad (4)$$

which correspond to the probability that, if we consider n of the hydrogen bonds made by molecule i in region k at time $t = 0$, all n hydrogen bonds are intact at time t irrespective of intermediate hydrogen bond breakage. The particular case of $n = 2$, corresponding to the correlation between pairs of hydrogen bonds, was applied by Raiteri et al.[6] to the study of correlations among hydrogen bonds in supercooled water. In the absence of correlations, at long times, $Q_k^n(t)$ factors into the single hydrogen bond correlation functions: $Q_k^n(t) \sim [Q_k^1(t)]^n$ ($Q_k^1(t)$ is the unnormalized $H_k(t)$), and a measure of correlation between the n hydrogen bonds of molecule i is the difference $\tilde{Q}_k^n(t) = [Q_k^1(t)]^n - Q_k^n(t)$. We calculate the correlation function $Q_k^n(t)$ and the normalized difference $G_k^n(t) = \tilde{Q}_k^n(t)/\tilde{Q}_k^n(0)$, and present our results in Figure 3 for $n = 2$ only, since correlations for $n > 2$ are very small under the ambient thermodynamic conditions of our simulations.

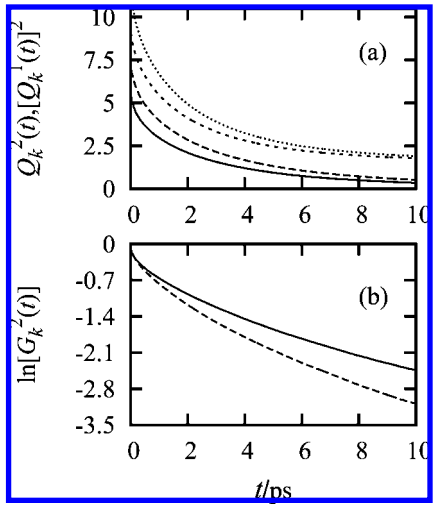

Figure 3. Time correlation functions for two nearest hydrogen bond neighbors in the laboratory frame: (a) $Q_k^2(t)$ for interfacial (solid line) and bulk (small dashes, shifted up by 1) water and $[Q_k^1(t)]^2$ for interfacial (large dashes) and bulk (dotted line, shifted up by 1) water; (b) $G_k^2(t)$ for interfacial (solid line) and bulk (large dashes) water.

As is evident from Figure 3a, at long times, $Q_k^2(t)$ approaches $[Q_k^1(t)]^2$, indicating that the dynamics of two neighboring hydrogen bonds become independent at long times but differ at short times due to correlations between them. The normalized difference $G_k^2(t)$ is shown in Figure 3b and indicates a slowdown for interfacial water with respect to bulk. In order to quantify this difference, we identify the relaxation time in the same manner as for $H_k(t)$ and obtain values of 2.33 and 1.64 ps for interfacial and bulk water. For the water/hydrocarbon system, correlations in the dynamics of neighboring hydrogen bonds are increased only slightly with respect to bulk water.

As seen so far, the dynamics of a hydrogen bond are correlated with that of the neighboring hydrogen bonds. The local hydrogen bonding environment therefore affects hydrogen bond dynamics. From a structural viewpoint, the number of hydrogen bonds per molecule characterizes the local environment. Since hydrogen bond dynamics is associated with translational diffusion of one molecule, say A, into the first coordination shell of a central molecule, say B, and reorientation of A and B to form a new hydrogen bond,[10] changes in hydrogen bond dynamics could depend on the local coordination of B, the coordination of the incoming molecule A, or the local coordination of the A, B pair. The last possibility was ruled out in bulk water by MD simulations of SPC/E water.[3,22] Instead, we consider the possibility that the coordination of the central molecule, B, is a sensitive indicator of the change in dynamics between bulk and interfacial water. We calculate the correlation function $S_k^m(t)$ defined as

$$S_k^m(t) = \frac{\langle p_m(0)[h_{i,j}(t) - \tilde{h}_k][h_{i,j}(0) - \tilde{h}_k]\rangle}{\langle p_m(0)[h_{i,j}(0) - \tilde{h}_k]^2\rangle} \qquad (5)$$

where $S_k^m(t)$ is the probability that a molecule i in region k with m hydrogen bonds at $t = 0$ forms a hydrogen bond with molecule j at time $t = 0$ and the pair remains hydrogen bonded until time t irrespective of hydrogen bond breakage in the intermediate time, $p_m(0) = 1$ or 0 if the central molecule i forms m hydrogen bonds at time 0 or not.

The correlation functions, $S_k^m(t)$, are shown in Figure 4 for interfacial and bulk water for $m = 1,..., 5$. The estimated relaxation

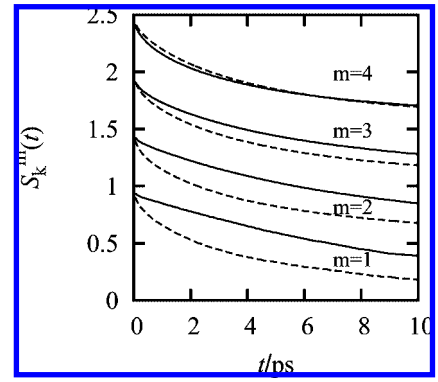

Figure 4. Hydrogen bond time correlation function, $C_m(t)$, for water at the interface (solid line) and in the bulk phase (large dashes) with coordination $m = 1$, $m = 2$ (shifted up by 0.5), $m = 3$ (shifted up by 1.0), and $m = 4$ (shifted up by 1.5) for the water/TMP system in the laboratory frame.

times (τ_r) for $m = 1-5$ in interfacial water are 11.06, 10.11, 7.49, 4.58, and 2.95 ps, and the corresponding values in bulk water are 4.49, 4.45, 4.61, 4.88, and 4.64 ps. For bulk water, τ_r is almost independent of the initial coordination and this can be expected in view of the independence on coordination of the two hydrogen bonded species for nonpolarizable models of water.[22] For interfacial water, the driving force for hydrogen bond dynamics is the need to form a tetrahedrally coordinated local structure and consequently an efficiently hydrogen bonded environment. Molecules with low coordination will therefore stay hydrogen bonded for a longer time depending on the deficit from tetrahedral coordination and availability of environments where four hydrogen bonds can be formed. This would explain the decrease in relaxation time from 11.06 to 4.58 ps corresponding to an increase in m from 1 to 4. In view of these m dependent relaxation times at the interface, the increase in relaxation time for the cooperativity correlation function $G_k^2(t)$ is reasonable.

The stretching exponent, γ_r, is close to 0.66 in the bulk for all m, indicating a similar relaxation mechanism. However, for interfacial water, γ_r has an approximately linear m dependence: $\gamma_r(m) = -0.13 + 1.10m$. For $m = 1$, $\gamma_r(1) \approx 1$ and exponential relaxation is observed. Since a singly coordinated molecule has no other neighboring water molecules, the question of correlated hydrogen bond dynamics does not arise and relaxation should be exponential. Unlike at the interface, a singly coordinated water molecule occurs transiently in bulk and consequently exhibits nonexponential relaxation. For $m \geq 1$, the stretching exponent for interfacial water deviates from 1, leading to increasingly nonexponential relaxation, possibly due to correlations.

C. Hydrogen Bond Dynamics and Translational Diffusion. Cooperative hydrogen bond formation and breakage can lead to nonexponential hydrogen bond relaxation. However, processes occurring on the same time scale as hydrogen bond dynamics can also lead to nonexponential decay. A hydrogen bond made by a central water molecule with another water molecule can break and reform if the latter does not diffuse away from the central molecule. Luzar and Chandler[2-4] identified translational diffusion as a possible contributor to nonexponential decay observed in hydrogen bond dynamics and formulated the rate of hydrogen bond formation and breakage as a kinetic process

$$A \underset{k_b}{\overset{k_f}{\rightleftharpoons}} B \qquad (6)$$

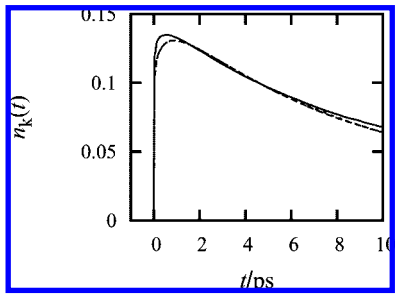

Figure 5. Time dependent probability that a pair of hydrogen bonded molecules at $t = 0$ are not bonded but reside within the first coordination shell at time t for interfacial (solid), intermediate (large dashes), and bulk water (small dashes) for the water/TMP system in the laboratory frame.

where A corresponds to a tagged pair of hydrogen bonded molecules, B is the product state that includes nonbonded pairs of water molecules that were initially bonded but remain within the first coordination shell (defined as $r_{AB} < 3.5$ Å) of each other, k_f is the rate constant for hydrogen bond dissociation (i.e., inverse of the hydrogen bond (HB) lifetime, $1/\tau_{HB1}$), and k_b is the rate constant of hydrogen bond reformation.

The reaction kinetics in region k is then described by

$$K_k(t) = -\frac{dH_k(t)}{dt} = k_f H_k(t) - k_b n_k(t) \qquad (7)$$

where $-K_k(t)$ is the reactive flux correlation function and corresponds to the average rate of change of hydrogen bond population where the bond between a tagged pair of molecules is broken at a time t later. We have defined $H_k(t)$ in eq 2 and define $n_k(t)$ as the probability that a bond that existed at $t = 0$ is broken and the molecules stay within the first coordination shell at time t. The following can be used to calculate $n_k(t)$:

$$n_k(t) = \frac{\langle [h_{i,j}(0) - \tilde{h}_k]\{1 - [h_{i,j}(t) - \tilde{h}_k]\}P_{i,j}(t)\rangle}{\langle h_{i,j}(0) - \tilde{h}_k\rangle} \qquad (8)$$

where $P_{i,j}(t) = 1$ or 0 depending on whether the tagged pair is within the first coordination shell of each other or not. A value of zero for $n_k(t)$ implies that the two molecules are either bonded or outside the first coordination shell and a nonzero values corresponds to the molecules being nonbonded but inside the first coordination shell.

The correlation functions $n_k(t)$ for water in each zone of the water/TMP system are presented in Figure 5. While the qualitative features of the interfacial and bulk water correlation functions are similar, at short times, interfacial water has a larger value of $n_k(t)$, indicating a higher probability that a water molecule is nonbonded but within the first coordination shell of another water molecule. Since at the interface a higher percentage of neighbors within the first coordination shell are hydrogen bonded,[13] compared to bulk, and in view of slower diffusion away from the interface,[19] a pair of initially hydrogen molecules will likely remain within the first coordination shell for a longer time. The long-time behavior is almost identical for interfacial and bulk water, perhaps due to diffusion setting in. The correlation functions for bulk and intermediate regions are identical, just as observed for single molecule relaxation.[19]

We calculate the numerical derivative of $H_k(t)$ to obtain $K_k(t)$ and present our results in Figure 6a. In addition to the initial

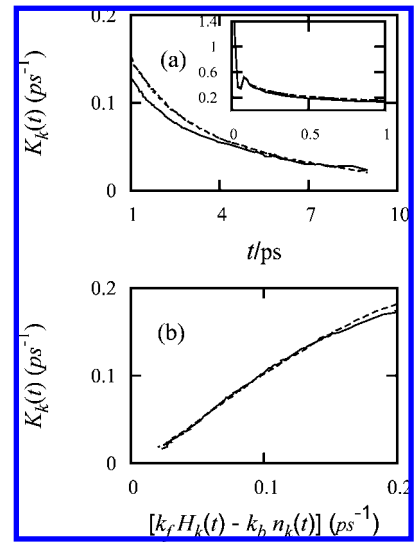

Figure 6. Rate of relaxation to equilibrium, $K_k(t)$ (ps^{-1}): (a) for interfacial (solid), intermediate (large dashes), and bulk (small dashes) water for the water/TMP system in the laboratory frame; (b) comparison with the rate equation (eq 7).

TABLE 2: Best Fit Parameters for the Kinetics of Hydrogen Bonding

	bulk	intermediate	interfacial
k_f (ps^{-1})	0.38	0.38	0.44
k_b (ps^{-1})	1.03	1.01	1.90
τ_{HB1} (ps)	2.61	2.61	2.27

inertial decay, an important short-time contribution to $K_k(t)$ is due to librations occurring on the time scale of 0.1−0.2 ps, as can be seen in the inset of Figure 6a. The short-time behavior of $K_k(t)$ for bulk and interfacial water is similar, indicating that the local environment does not affect the librational contribution to hydrogen bond dynamics. If each hydrogen bond acted independently of the other hydrogen bonds, the long time decay of $K_k(t)$ would be exponential, $K_k(t) \simeq \nu_k \exp(-\nu_k t)$, and $1/\nu_k$ could be identified as the average hydrogen bond lifetime for region k. In the present case, since $H_k(t)$ is well represented by eq 3, $K_k(t)$ exhibits nonexponential decay at long times.

To test the diffusion model, the best fit values of k_f and k_b are obtained by minimizing squared deviation between the left- and right-hand sides of eq 7. The parameters obtained from this fit are summarized in Table 2. For bulk water, the best fit value of k_f is 0.38 ps^{-1} and similar to the value, 0.35 ps^{-1}, obtained for the same water model by Xu et al.[22] The value of k_f increases slightly to 0.44 ps^{-1} at the interface, indicating a faster breakage of hydrogen bonds. However, the rate of the backward reaction increases by a larger amount, from 1.03 to 1.90 ps^{-1}, and the time required for hydrogen bond reformation decreases. The net effect is the apparent increase in relaxation time, τ_r, for $H_k(t)$. This is expected, since the diffusion coefficient perpendicular to the interface is smaller at the interface than in the bulk[19] and water molecules are more likely to stay inside the first coordination shell at the interface. The validity of the diffusion model (eq 7) is demonstrated in Figure 6b by plotting $K_k(t)$ vs $k_f H_k(t) - k_b n_k(t)$ for the long times where $K_k(t) \geq 0.20$ ps^{-1}, as this represents the time scale on which the diffusion model is best applicable. The data should be compared with a straight line of unit slope, and the fit performs the best for $K_k(t) \leq 0.15$ ps^{-1} corresponding to $t \geq 1.1$ ps. For shorter times, the agreement is worse and the data points start deviating from the unit slope line for $K_k(t) \geq 1.5$. The nonexponential behavior of

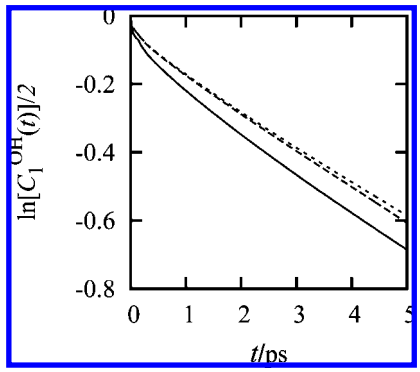

Figure 7. Orientational time correlation function for the O−H vector in the interfacial (solid), intermediate (large dashes), and bulk water (small dashes) for the water/TMP system in the laboratory frame.

the hydrogen bond TCF $H_k(t)$ can therefore be rationalized in terms of diffusion of water molecules coupled with hydrogen bond formation and breakage.

The inverse of the forward rate constant in eq 7 represents a hydrogen bond lifetime, $\tau_{HB1} = 1/k_f$, and these values are presented in Table 2. Luzar[2] has suggested using τ_{HB1}, rather than a decay time associated with $H_k(t)$ as the actual hydrogen bond lifetime, since in the kinetic model (eq 7) $1/k_f$ depends only on hydrogen bond dissociation. Selecting this criterion, we observe that the mean lifetime of a hydrogen bond actually decreases from 2.61 ps in the bulk to 2.27 ps at the interface when the effect of diffusion has been removed from the apparent slowdown of $H_k(t)$ at the interface. This represents a small change in hydrogen bond lifetimes and is consistent with our observations for translational diffusion and rotational relaxation at the interface.[19]

D. Hydrogen Bond Dynamics and O−H Reorientation. Since the angle between the O−H covalent bond and the H···O distance is a part of the hydrogen bond definition, reorientation of the O−H vector is expected to contribute to hydrogen bond formation and breakage. In this subsection, we examine the reorientation of this vector in interfacial water and the connection of its relaxation mechanism to hydrogen bond dynamics.

The orientational TCF for the O−H vector is defined as

$$C_l^{OH}(t) = \langle P_l[\hat{u}_{OH}(0)\cdot\hat{u}_{OH}(t)]\rangle \qquad (9)$$

where $P_l(x)$ is the Legendre polynomial of order l and $\hat{u}_{OH}(t)$ is the unit vector along the covalent O−H direction at time t.

$C_l^{OH}(t)$ is presented in Figure 7 for interfacial, intermediate, and bulk phases of the water/TMP system in the laboratory frame. The O−H vector reorients faster at the interface than in the bulk. The orientational relaxation times are calculated from fits of the long-time part of the TCF to an exponential and presented in Table 3 for $l = 1-3$. These orientational correlation times decrease from 4.6 ps in the bulk to 4 ps at the interface for $l = 1$. Their variation from bulk to interface follows the trend we observed earlier for the molecular H−H vector. For the unit vectors along the two other molecular principal axes of inertia, we found a slow-down in the interfacial region.[19] In view of the faster reorientation of the O−H vector, the hydrogen bond involving this vector is likely to break faster at the interface and this is supported by the hydrogen bond lifetimes presented in Table 2.

A key question about O−H rotational dynamics is whether it is composed of diffusive or large-angle jumps or a combination thereof. In our earlier work on the reorientation of the principal axes of the water molecule,[19] we found that the l dependence of orientational relaxation times could be best described by assuming that reorientation is comprised of large-angle jumps and diffusive rotational motion between the jumps. Furthermore, interfacial water exhibited anisotropic reorientation; i.e., the $t = 0$ orientation of the selected molecular vector with respect to the normal to the interface determined the orientational relaxation time for interfacial molecules. For example, molecules with their dipole moment vector oriented toward the hydrocarbon phases exhibited the slowest orientational relaxation followed by those with dipole vectors oriented such that one O−H bond pointed toward the hydrocarbon phase. All other orientations were associated with bulk-like orientational relaxation times.[19] Clearly, this observation violates one of the assumptions of isotropic relaxation that is implicit to both diffusive or large angular jump models for rotational dynamics[25,26] and consequently these models are not entirely applicable to interfacial dynamics.

As observed in section III.B, the relaxation of the hydrogen bond correlation function depends strongly on the local coordination. Since the number of hydrogen bonds made by a water molecule at the interface is related to its orientation at the interface, this suggests the possibility that perhaps hydrogen bond dynamics is also dependent on initial orientation (and implicitly the local coordination) of the O−H vector with respect to the interface. To test this possibility, we partition all interfacial O−H vectors into six subsets such that the O−H vectors in subset n_θ are oriented in the angular range $[\theta_0, \theta_0 + 30]$, where $\theta_0 = 30(n_\theta - 1)$ and $n_\theta = 1,..., 6$, with respect to the normal to the interface. Orientational $l = 1$, $C_{n_\theta}^{OH}(t)$, and the hydrogen bond correlation functions, $C_{n_\theta}(t)$, are calculated for molecules that belong to each n_θ analogous to eqs 9 and 2 but with the restriction that at $t = 0$ the O−H vector is in the selected angular range.

Since the orientation of molecules at the interface is likely to be correlated with the local orientation of the aqueous surface due to capillary wave fluctuations, averages for angular subsets are more likely to be affected by capillary waves than averages involving all angles. Consequently, we minimize the effect of these surface fluctuations by calculating the TCFs for each angular subset in the intrinsic frame only.

The TCFs obtained for each angular subset at the interface are presented in Figure 8 and indicate significant dependence of orientational relaxation on the $t = 0$ orientation at the interface. Clearly, O−H reorientation is anisotropic at the interface. If hydrogen bond dynamics depends on the orientation of the O−H vector, we should see a corresponding anisotropy in the hydrogen bond TCF. From Figure 8b, it appears that the

TABLE 3: O−H Orientational Relaxation Times at the Interface and in the Bulk

	bulk					interfacial				
	τ_1 (ps)	τ_2 (ps)	τ_3 (ps)	τ_1/τ_2	τ_1/τ_3	τ_1 (ps)	τ_2 (ps)	τ_3 (ps)	τ_1/τ_2	τ_1/τ_3
molecular dynamics	4.6	2.2	1.5	2.1	3.1	4	2.2	1.6	1.8	2.5
O−O reorientation between switches	13.3	5.8	3.6	2.3	3.7	10.6	5.5	3.5	1.9	3
O−H hop from eq 10	7	3.5	2.6	2.0	2.7	6.4	3.7	2.9	1.7	2.2

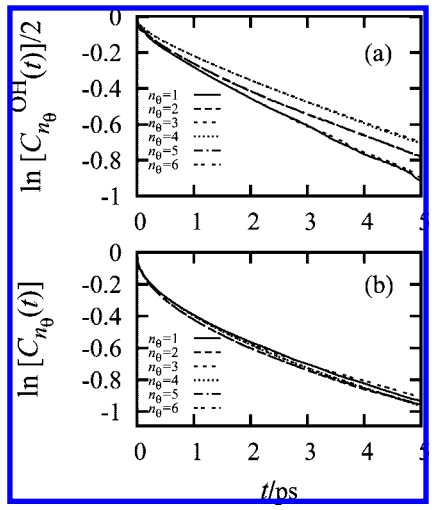

Figure 8. Initial orientation dependence in the intrinsic frame for (a) the O−H orientational time correlation function, $C_{n_\theta}^{OH}(t)$, for $l = 1$ and (b) the hydrogen bond correlation function, $C_{n_\theta}(t)$, for O−H vectors in the angular subset $n_\theta = 1$ (solid line), 2 (large dashes), 3 (small dashes), 4 (dotted line), 5 (large dash−dot), and 6 (pair of short dashes).

TABLE 4: Dependence of Orientational and Hydrogen Bond Relaxation Times (in Picoseconds) on Initial Molecular Orientation

	$n_\theta = 1$	$n_\theta = 2$	$n_\theta = 3$	$n_\theta = 4$	$n_\theta = 5$	$n_\theta = 6$
$\tau_{n_\theta}^{OH}$	3	3.6	4	3.9	3.6	3.1
τ_{n_θ}	5.9	5.2	4.8	4.8	5.3	5.3

hydrogen bond TCFs are more weakly dependent on the initial orientation of the O−H vector at the interface.

To quantify the relaxation times for O−H reorientation and hydrogen bond dynamics, the relaxation times for rotational motion, $\tau_{n_\theta}^{OH}$, and hydrogen bond relaxation times, τ_{n_θ}, are obtained from the following fit: $C_{n_\theta}^{OH}(t) \propto \exp\{-t/[2\tau_{n_\theta}^{OH}]\}$ and $C_{n_\theta}(t)$ is fit to eq 2 and presented in Table 4.

For all angular subsets, there is an apparent inverse correlation between $\tau_{n_\theta}^{OH}$ and τ_{n_θ}. There is an increase in $\tau_{n_\theta}^{OH}$ from $n_\theta = 1$ to 3 and a decrease to $n_\theta = 6$, and the variation is symmetric about $\theta = \pi/2$. Correponding to this change in orientational relaxation times, the hydrogen bond relaxation time decreases from 5.9 to 4.8 ps on going from $n_\theta = 1$ to 3 and increases beyond this angular subset.

In previous work,[13] we found that the O−H vector adopts two preferred orientations at the interface, one pointing toward the hydrocarbon phase and the second in the plane of the interface. These two scenarios correspond to angular subsets of $n_\theta = 1$ and $n_\theta = 3$ and 4. The orientational relaxation time is smallest for $n_\theta = 1$ and 6, and the hydrogen bond relaxation time is the longest. Such an orientation, while preferred at the interface, does not have a long lifetime possibly due to the need of the water molecule to be involved in a tetrahedral local environment. Faster reorientation should lead to faster hydrogen bond dynamics, but this is not the case. For $n_\theta = 3$ and 4, the orientational relaxation times are the longest while the hydrogen bond relaxation times are the shortest. In view of the τ_{n_θ} value of 4.8 ps for $n_\theta = 3$ or 4, this suggests that these molecules are the primary contributions to hydrogen bond dynamics.

While an analysis of O−H reorientations is informative, it does not shed any light on the mechanism of hydrogen bond formation or breakage. Laage and Hynes[10] proposed a mechanism of reorientation in bulk water in which the covalent O−H bond undergoes a jump of 60° from one hydrogen bond accepter (O^a) to another (O^b), thereby leading to hydrogen bond breakage and reformation. In between the angular hops, the O−H vector exhibits a slow reorientation along with the hydrogen bonded network. This slow reorientation can be understood in terms of the coupling of the O−H vector to the $O\cdots O^a$ axis. To verify that this is indeed the case for our system, the hydrogen bonding criterion is extended to include all molecular pairs with O···O distances smaller than 4.0 Å and HOO angles smaller than 50°. In this new ensemble, O−H and O···O orientational TCFs are calculated for $l = 1-3$ between hydrogen bond switching events and presented in Figure 9a. There is a clear correlation between the O−H and O···O reorientations between hydrogen bond switching events, since the long-time decay for both is similar. Even with this extended hydrogen bonding criterion, reorientation is slower at the interface than in the bulk, just as for the initial criterion.

Corresponding to this physical picture of hydrogen bond dynamics, Laage and Hynes[10] proposed that relaxation can be approximated as independent steps in the overall reorientation of the O−H vector and obtained the following expression for the orientational relaxation time

$$\frac{1}{\tau_l^{OH}} = \frac{1}{\tau_l^{jump}} + \frac{1}{\tau_l^{OO}} \tag{10}$$

where τ_l^{OH} is the exponential decay time for the O−H vector in the laboratory frame and τ_l^{OO} is the corresponding time for the O···O vector between hydrogen bond switches for the lth order Legendre polynomial. Since the O−H vector jumps from O^a to O^b, the angular jump can be characterized by a jump angle θ_0 and the frequency of these jumps, $1/\tau_0$ and the lth order characteristic jump times, τ_l^{jump}, can be calculated based on the Ivanov model

$$\frac{\tau_0}{\tau_l^{jump}} = 1 - \frac{1}{2l+1}\frac{\sin[(l+1/2)\theta_0]}{\sin(\theta_0/2)} \tag{11}$$

The detailed mechanism of hydrogen bond reformation and the average jump angle, θ_0, can be obtained by following the hydrogen bond donor and the acceptor molecules between which the hydrogen bond hops.[10] Near the interface, O−H reorientation is restricted by the presence of the hydrocarbon phase, and geometrical restrictions should be accounted for in the analysis of orientation relaxation times.[27] Instead of doing so, we assume that the model of Laage and Hynes[10] is applicable to our system and our objective is therefore to extract the parameters θ_0 and τ_0 from eqs 10 and 11. The relaxation times, τ_l^{OH}, have already been calculated and presented in Table 3. We fit the time dependence of the O···O orientational correlation function between hops in the time range 1.5 ps $< t <$ 5.0 ps and present the corresponding relaxation times for $l = 1-3$ in Table 3. In order to determine the deviation from the small angular step diffusion model, we calculate the ratios τ_1/τ_2 and τ_1/τ_3 for the O···O rotation and obtain values of 2.4 and 3.9. These magnitudes are different from the values of 3 and 6 expected from the rotational diffusion model and deviate from the values of 3.0 and 5.5 obtained by Laage and Hynes for bulk water. A possible source of this difference might be the different simulation protocols used in this work and by Laage and Hynes.[10]

With the calculated values of τ_l^{OH} and τ_l^{OO}, we use eq 10 to obtain the l dependence of τ_l^{jump} and these are reported in Table

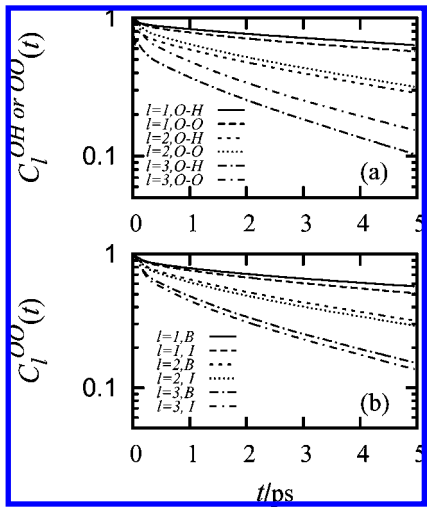

Figure 9. Orientational time correlation functions for (a) O−H and O···O reorientation between hydrogen bond switches for $l = 1-3$ and (b) O···O reorientation between bond switches for $l = 1-3$ at the interface (I) and in the bulk (B).

3. With these values of τ_l^{jump} available for $l = 1$ and 2, eq 11 leads to values of $\theta_0 = 64°$ and $\tau_0 = 2.7$ ps. The magnitude of the angular jump is in reasonable agreement with the value of 60°, although the hydrogen bond switching time scale of 2.7 ps exceeds the value of 1.8 ps obtained by Laage and Hynes[10] for bulk water. We note that τ_0 is in good agreement with the average hydrogen bond lifetime, τ_{HB1}, obtained from the kinetic model of Luzar and Chandler[3] (presented in Table 2), and this perhaps allows for a connection between the pair diffusion and O−H reorientation models.

As shown in section III.B, the hydrogen bond relaxation time depends strongly on the local coordination. O−H reorientation is likely to also be a function of local coordination. A local environment dependent mechanism of O−H reorientation is likely to exist at the interface, and the original Laage−Hynes model[10] would need to be modified for reorientation of water near interfaces. With this caveat, we apply the Laage−Hynes[10] model to interfacial orientational relaxation and obtain values of $\theta_0 = 84°$ and $\tau_0 = 3.9$ ps. The magnitude of the angular jump is larger than in the bulk and might be the result of confinement at the interface. The value of τ_0 is larger than the average hydrogen bond lifetime estimate of 2.1 ps (Table 2), and indicates slower hydrogen bond switching at the interface than in the bulk. This result is consistent with the slower hydrogen bond dynamics at the interface observed in section III.A. The discrepancy between τ_{HB1} and τ_0 is likely a consequence of anisotropic dynamics at the interface.

IV. Summary

MD simulations were performed for water/hydrocarbon interfaces and the trajectories analyzed in order to study hydrogen bond dynamics. Hydrogen bond TCFs were found to decay nonexponentially, with interfacial water molecules exhibiting slower relaxation than bulk water. We carried out additional data analysis to determine the mechanism of hydrogen bond breakage and reformation in order to elucidate this behavior. Several factors contributing to hydrogen bond relaxation mechanism were examined.

The first one was cooperativity of hydrogen bond dynamics, which can lead to multiple time scales. A study of the cooperativity of hydrogen bond dynamics of pairs of hydrogen bonds made by one molecule revealed an increase in cooperativity at the interface compared to the bulk. Hydrogen bond relaxation times were found to be strongly dependent on the local coordination, with an increase in coordination from 1 leading to deviation from exponential decay.

A second possible source of nonexponential hydrogen bond relaxation is the coupling of hydrogen bond dynamics to diffusion. The kinetic model of Luzar and Chander[3] relating hydrogen bond dynamics to hydrogen bond breakage and reformation was successfully tested for both bulk and interfacial systems. The time scale for hydrogen bond breakage was found to decrease at the interface compared to the bulk, while the rate of reformation increases at the interface due to slower translational diffusion normal to the interface. The net effect is a longer relaxation time for interfacial water. Thus, nonexponential relaxation appears to be a result of cooperativity as well as of translational diffusion.

Since O−H reorientation is involved in hydrogen bond formation and breakage, we calculated the orientational TCFs of this vector and found that it reorients faster at the interface than in the bulk. This observation would be counterintuitive, since we find hydrogen bond relaxation times to be longer at the interface than in the bulk. However, a better comparison is not with the hydrogen bond relaxation times but with the hydrogen bond lifetimes calculated from the kinetic analysis and we find that faster O−H reorientation is associated with faster hydrogen bond breakage as expected.

At the interface, O−H reorientation is anisotropic and the $l = 1$ orientational TCF depends on the $t = 0$ orientation of the O−H vector. While we also find anisotropy in hydrogen bond TCF, it appears to be weak and inversely correlated with orientational relaxation.

The contribution of O−H reorientation to hydrogen bond breakage was inferred on the basis of the approach of Laage and Hynes.[10] We found that O−H reorientation is coupled to a slow reorientation of the O···O vector made with the hydrogen bond acceptor, as suggested by Laage and Hynes. This O···O reorientation is slower at the interface than in the bulk, since the interface is a confined environment. For bulk water, we estimate that, with respect to the O···O frame, the O−H vector makes an angular jump of ∼60° from one hydrogen bond acceptor to another. The time scale for this hydrogen bond switching is comparable to the hydrogen bond lifetime obtained from the kinetic model. Given the anisotropy of dynamics at the interface, this bulk-phase model is only approximate. With this caveat, we estimate an angular jump of 84° and a hydrogen bond switching time of 3.9 ps, which is much larger than the hydrogen bond breakage time calculated from the kinetic model. Models for rotational dynamics that include restrictions on the range of angular motion are therefore needed to analyze the reorientation of molecules at the interface.[27]

The effect of hydrocarbon branching on hydrogen bond dynamics was found to be minimal. From the point of view of understanding the properties of interfacial water near biomolecules, it would be worth exploring this connection between local molecular orientation and dynamics for aqueous interfaces where the polarity of the nonaqueous phase can be varied systematically.

Acknowledgment. This work was supported by the NSF Grant CHE 0608640 and the DOE Grant DE-FG03-0ZER15376.

References and Notes

(1) Geiger, A.; Kleene, M.; Paschek, D.; Rehtanz, A. *J. Mol. Liq.* **2003**, *106*, 131.
(2) Luzar, A. *J. Chem. Phys.* **2000**, *113*, 10663.
(3) Luzar, A.; Chandler, D. *Nature* **1996**, *379*, 55.
(4) Luzar, A.; Chandler, D. *Phys. Rev. Lett.* **1996**, *76*, 928.
(5) Paschek, D.; Geiger, A. *J. Phys. Chem. B* **1999**, *103*, 4139.
(6) Raiteri, P.; Laio, A.; Parrinello, M. *Phys. Rev. Lett.* **2004**, *93*, 087801.
(7) Starr, F. W.; Nielsen, J. K.; Stanley, H. E. *Phys. Rev. E* **2000**, *62*, 579.
(8) Auer, B.; Kumar, R.; Schmidt, J. R.; Skinner, J. L. *Proc. Natl. Acad. Sci.* **2007**, *104*, 14215.
(9) Loparo, J. J.; Roberts, S. T.; Tokmakoff, A. *J. Chem. Phys.* **2006**, *125*, 194522.
(10) Laage, D.; Hynes, J. T. *Science* **2006**, *311*, 832.
(11) Errington, J. R.; Debenedetti, P. G.; Torquato, S. *Phys. Rev. Lett.* **2002**, *89*, 215503.
(12) Benjamin, I. *J. Phys. Chem. B* **2005**, *109*, 13711.
(13) Chowdhary, J.; Ladanyi, B. M. *J. Phys. Chem. B* **2006**, *110*, 15442.
(14) Jedlovszky, P. *J. Phys.: Condens. Matter* **2004**, *16*, S5389.
(15) Liu, P.; Harder, E.; Berne, B. J. *J. Phys. Chem. B* **2005**, *109*, 2949.
(16) Paul, S.; Chandra, A. *Chem. Phys. Lett.* **2004**, *386*, 218.
(17) Chanda, J.; Bandyopadhyay, S. *J. Phys. Chem. B* **2006**, *110*, 23443.
(18) Hanasaki, I.; Nakatani, A. *J. Chem. Phys.* **2006**, *124*, 174714.
(19) Chowdhary, J.; Ladanyi, B. M. *J. Phys. Chem. B* **2008**, *112* 6259.
(20) Berendsen, H. J. C.; Grigera, J. R.; Straatsma, T. P. *J. Phys. Chem.* **1987**, *91*, 6269.
(21) Jorgensen, W. L.; Madura, J. D.; Swenson, C. J. *J. Am. Chem. Soc.* **1984**, *106*, 6638.
(22) Xu, H.; Stern, H. A.; Berne, B. J. *J. Phys. Chem. B* **2002**, *106*, 2054.
(23) Buff, F. P.; Lovett, R. A.; Stillinger, F. H. *Phys. Rev. Lett.* **1965**, *15*, 621.
(24) Chowdhary, J.; Ladanyi, B. M. *Phys. Rev. E* **2008**, *77*, 031609.
(25) Ivanov, E. N. *Sov. Phys. JETP* **1964**, *18*, 1041.
(26) Valiev, K. A.; Ivanov, E. N. *Sov. Phys. Usp.* **1973**, *16*, 1.
(27) Laage, D,; Hynes, J. T. Submitted for publication.

JP8061509